International Journal of Applied Pharmaceutics

ISSN- 0975-7058 Vol 18, Issue 1, 2026

Original Article

GREEN SYNTHESIS OF ZINC OXIDE NANOPARTICLES OF *TRADESCANTIA SPATHACEA* PLANT

SHANKARAIAH PULIPAKA[1], ASHISH SUTTEE[2*], V. JYOTHI[3], R. VANI[3]

[1*]Department of Pharmacognosy, Geethanjali College of Pharmacy, Cheeryal, Keesara, Medchal, Hyderabad-501301, Telangana, India. [2*]School of Pharmaceutical Sciences, Lovely Professional University, Punjab, India. [3]Shadan Women's college of Pharmacy. Khairathabad, Hyderabad, Telangana-500004, India

*Corresponding author: Ashish Suttee; *Email: ashish7sattee@gmail.com

Received: 29 May 2025, Revised and Accepted: 15 Oct 2025

ABSTRACT

Objective: In this investigation, we worked to determine whenever herbal nanoparticle formulations made from methanolic extracts of *Tradescantia spathacea* (T. S.) leaves exhibited any acute toxicity.

Methods: Male and female mice (n = 5 per group per sex) received dosages of 500, 1000, 2000, 3000, and 5000 mg/kg of T. S. methanolic extract containing zinc oxide (ZnO) nanoparticles. Over the course of 14 d, the mice were studied for changes in behavior and weight, as well as death. Vital organs were also subjected to histological examination.

Results: Toxicological symptoms and a 10-30% death rate were caused by doses of 3,000 mg/kg and 5,000 mg/kg, respectively. No side effects were seen at dosages of 1000 mg/kg and 2000 mg/kg. No notable morphological alterations in critical organs were detected during histopathological investigation. The lipid profiles and hypoglycaemic effects were improved by all dosages that were evaluated.

Conclusion: According to the results, therapeutic dosages of T. S. ZnO nanoparticles are safe, even at an LD50 greater than 5000 mg/kg. Traditional therapeutic uses of *Tradescantia spathacea* are now well-supported by the results. Histopathological analyses revealed no significant morphological changes in vital organs.

Keywords: *Tradescantia spathacea*, Acute toxicity, Methanolic extract, ZnO nanoparticles, Hypoglycemic effect, Toxicological profile, Histopathological analyses

DOI: https://dx.doi.org/10.22159/ijap.2026v18i1.55279 Journal homepage: https://innovareacademics.in/journals/index.php/ijap

INTRODUCTION

Over the last decade, extensive research has focused on metal oxide nanoparticles (NPs) due to their significant roles in both basic and applied sciences. Biological processes involving microorganisms, enzymes, plants, and algae have emerged as viable, eco-friendly alternatives to conventional, hazardous, and costly chemical and physical methods for nanoparticle synthesis. These approaches offer sustainability while maintaining efficiency [1-4]. Nanoparticles, particularly those made from metals and metal oxides, have captured the attention of researchers across various fields, including biology, chemistry, physics, medicine, and engineering. This interest arises primarily from their high surface area and distinctive properties, including antimicrobial, magnetic, electrical, and catalytic activities [5]. Zinc oxide nanoparticles (ZnO NPs) are particularly interesting. They possess a wide bandgap of 3.3 eV at room temperature and exhibit strong exciton-binding energy of 60 meV, enabling them to have photochemical, photocatalytic, UV-filtering, and antibacterial properties [6]. The ability of certain oxides to inhibit microbial growth is well-documented, with studies showing that materials like CaO, MgO, and ZnO exhibit antibacterial properties, often due to the generation of reactive oxygen species on their surfaces [7, 8].

Plant extracts offer an environmentally friendly approach to synthesizing metal oxide nanoparticles, facilitating the controlled production of nanoparticles with well-defined sizes and shapes [9, 10]. This environmentally friendly synthesis method eliminates harmful organic solvents and extreme reaction conditions. Moreover, the incorporation of stabilizing and capping agents has enabled the formation of nanostructures in aqueous media, making the process safer and more sustainable [11-15]. *Tradescantia spathacea*, a plant rich in bioactive compounds such as flavonoids, terpenoids, phenols, saponins, alkaloids, and vitamins, was chosen for this study due to its numerous pharmacological properties, including anti-inflammatory, antioxidant, antifungal, antibacterial, anti-diarrheal, anti-ulcer, and anti-hypertonic activities. It mainly consists of two new compounds, (±) tradescantia (13) and tradescantoside, along with fourteen known compounds from the aerial parts of *Tradescantia spathacea Sw*. (Commelinaceae). They are promising agents for treating type 2 diabetes. The plant's potential to facilitate the synthesis of metal oxide nanoparticles in an aqueous medium further underscores its value as a natural, renewable, and cost-effective resource, eliminating the need for harmful materials or toxic solvents [16-23].

This research explores the preparation and stabilization of ZnO nanoparticles using *Tradescantia spathacea* extracts. Advanced characterization techniques such as X-ray diffraction (XRD) and scanning electron microscopy (SEM) were utilized to examine the crystal structure and surface morphology of the synthesized nanoparticles, offering a comprehensive insight into their properties and potential applications.

METHODS AND MATERIALS

Materials

Zinc nitrate hexahydrate ($Zn(NO_3)_2 \cdot 6H_2O$) was procured from SR Life Science Pvt. Ltd., Hyderabad, ensuring the use of analytical-grade compounds throughout the study. Fresh *Tradescantia spathacea* (T. S.) and voucher number is BSI/DRC/2020-21/identification/Tech/66, plants were collected during the summer months of May and June from Hyderabad, Telangana, India. The plant specimens were verified by P. V. Prasanna, a Scientist "G" and the Head of Office at the Deccan Regional Centre of the Botanical Survey of India, located in Hyderabad, Telangana. A voucher specimen was prepared as proof of authentication and is securely stored for future reference. Streptozotocin, a key chemical used in the study, was also obtained from SRL Private Limited, Hyderabad.

Preparation of extracts

Extraction, as the term is used pharmaceutically, involves the separation of medicinally active portions of plant or animal tissues from the inactive or inert components by using selective solvents in standard extraction procedures. The products obtained from plants are typically impure liquids, semisolids, or powders intended for

oral or external use only. The leaves of the plant were thoroughly cleaned and dried in a dust-free oven at 30 °C. Once dried, the leaves were powdered to prepare them for extraction. The powdered leaves were then mixed with the solvent using ultrasonic frequencies ranging from 20 to 2000 kHz. After the extraction, the purified extract is prepared for the preparation of nanoparticles. This ultrasound-assisted extraction technique, driven by sound-induced cavitation, enhances the interaction between the solvent and the sample while increasing the permeability of cell walls. This method offers a simple, cost-effective solution suitable for both small-and large-scale phytochemical extractions. The methanolic extract of the leaves was subsequently separated using Whatman No. 1 filter paper. The resulting extract was either utilized immediately for the synthesis of ZnO nanoparticles or stored at 0 °C for future studies. This efficient process ensures the preservation of the phytochemicals for subsequent applications [24-26].

ZnO nanoparticle synthesis

The synthesis process required stirring 25 ml of plant extract with 0.1 M zinc nitrate hexahydrate for two hours. After allowing the reaction mixture to cool for 24 h, the resulting precipitate was separated by centrifugation at 6000 rpm for 15 min. The precipitate was washed several times with deionized water to eliminate impurities and then dried at 80 °C. The dried material was heated in a muffle furnace at 350 °C for three hours. After cooling, 5 µl of the ZnO nanoparticle solution was applied to a carbon-coated copper grid. This sample was then analyzed using a scanning electron microscope (SEM) to examine its structural and morphological characteristics [27].

Nanoparticles' characteristics

The shape, average particle size, and functional group analysis of ZnO nanoparticles (NPs) derived from *Tradescantia spathacea* (T. S.) were genetically engineered. Several characterization techniques, including scanning electron microscopy (SEM), zeta potential analysis, particle size analysis, and X-ray diffraction (XRD), were employed to identify and evaluate nanoparticles synthesized using green methods. The crystalline size of T. S. ZnO NPs was determined through X-ray diffraction measurements conducted over a 2θ range of 20°-80°. Particle size and zeta potential were assessed using a particle size analyzer, which also helped evaluate the dispersion properties of the nanoparticles. To identify the biomolecules involved in the synthesis of T. S. ZnO nanoparticles, Fourier transform infrared (FTIR) spectroscopy was conducted over a range of 400 to 4000 cm^{-1}. SEM was utilized to investigate the morphology, particle size, shape, and elemental composition of T. S. ZnO nanoparticles, offering detailed insights into their structure and characteristics [28, 29].

Particle size and zeta potential

The particle size and zeta potential were measured using Malvern Instruments' Dynamic Light Scattering (DLS) method. The measurements were taken at a fixed angle of 90° and an average temperature of 25 °C. The nanoparticle suspension was sonicated in distilled water for six minutes. Zeta potential data were obtained by electrophoretic light scattering at 25 °C and 150 V. The zeta potential plays a crucial role in stabilizing the formulation by influencing charge conductivity [30, 31].

FTIR spectroscopy

FT-IR analysis was conducted after centrifuging the reaction solution at 6000 rpm for 15 min. The resulting pellets were washed multiple times with 20 ml of distilled water to remove any impurities. After drying, the substance was crushed with KBr and prepared for analysis. The samples were then measured using a Shimadzu 8400S, with a spectral range of 500–4000 cm^{-1} and a resolution of 4 cm^{-1}. The FTIR spectrum of the leaf extract was examined following nanoparticle synthesis to identify the functional groups involved in the formation of T. S. ZnO nanoparticles. The peak values in the FTIR spectrum were recorded and analyzed, with readings taken twice to ensure accuracy and reliability [32, 33].

XRD analysis

Powder X-ray Diffraction (XRD) is a vital characterization technique in solid-state science and materials research, primarily used by mineralogists and solid-state chemists to investigate the physicochemical composition of unknown materials. XRD allows for the rapid identification of a compound's unit cell by analyzing the size, shape, structural parameters, and phase fractions. The diffraction pattern's peak positions provide valuable information about the unit cell's translational symmetry, including its size and shape. In this study, XRD was employed to examine the structural properties of the synthesized nanoparticles. The nanoparticles were analyzed using a PAN analytical X-ray diffractometer set at 4000V and 20mA, with the scanning range from 20° to 80° at a scanning rate of 0.02°/min. The crystal structures of the materials were refined to determine accurate atomic positions [34, 35].

Scanning electron microscopy (SEM) analysis

Scanning Electron Microscopy (SEM) works on similar principles to light reflection microscopes, but instead of light, it uses an electron beam to create images. When the electron beam strikes an object, the electrons are reflected, and this reflection is captured by a detector to form an image. In this study, plant extracts were used as capping agents to synthesize nanoparticles, and SEM was employed to observe their morphology and surface characteristics [36, 37].

Acute toxicity study

We conducted acute toxicity tests following the OECD Guidelines 425. These guidelines explain how to evaluate the harmful effects of substances on living organisms. Male and female albino mice (GCPK/IAEC/2020-21/01), aged 8 to 10 w with average body weights of 28±4 g, were selected for the study. The mice were randomly assigned to different groups, as outlined in table 1. Prior to the dose administration, the mice were fasted for 3 to 4 h, but water was made available to them at all times. Each group of mice received an oral dose of 2000 mg/kg, based on the body weight of a single mouse [38]. The animal were closely monitored for the first 30 min and then for the next 4 h after the dose was given, for any signs of toxicity. After a few hours, the mice were given food again. Four additional mice were administered the same dose to assess the endurance of the drug-treated mice. The vehicle control group received the same treatment following the procedure.

Table 1: OECD 425 guidelines for acute toxicity

Group	Treatment	Drug concentration and route of administration	Number of animals (Mice)
I	Vehicle control (1% w/v CMC)	1% w/v carboxymethyl cellulose, orally (p. o.)	5
II	ZONP	2000 mg/kg, orally (p. o.)	5
III	TSLE	2000 mg/kg, orally (p. o.)	5
IV	TSLE+ZONP	2000 mg/kg, orally (p. o.)	5

CMC: Carboxy Methyl Cellulose; ZONP: Zinc Oxide Nanoparticles; TSLE: *Tradescantia spathacea Leaf Extract;* TSLE ZONP: *Tradescantia spathacea Leaf Extract* Zinc Oxide Nanoparticles

The different groups were closely monitored for any adverse side effects throughout the study. Behavioural characteristics were recorded at various time intervals: the first 30 min, 4 h, 24 h, and then at regular intervals over the next 14 d. The body weight of the mice was measured several times during this period. At the end of the experiment, the mice were anesthetized with diethyl ether, and after euthanasia, their kidneys, liver, and heart were carefully dissected. The organ weights were recorded, and blood samples

were collected via heart puncture for biochemical and haematological analysis. The blood samples were then sent to the pathology lab, while the organs were preserved in 10% formalin solution for histological examination [38-40]

Biochemical evaluation

Blood samples were analyzed for parameters such as blood sugar, cholesterol, triglycerides, HDL, LDL, VLDL, creatinine, urea, bilirubin, alkaline phosphatase, total proteins, globulins, and albumin [41].

Blood analysis

Blood samples in EDTA tubes were analyzed for CBC parameters, including total RBC count, hemoglobin, MCH, MCV, MCHC, WBC count, platelet count, and differential counts of lymphocytes, eosinophils, neutrophils, basophils, and monocytes [41].

Histopathological investigation

The heart, liver, and kidneys of the mice were sent to the pathology department at Kakatiya Medical College, Warangal, Telangana, for histological examination. The organs were carefully fixed in paraffin wax, and 5 mm tissue sections were stained with eosin and hematoxylin. The tissue structures were examined using a light microscope, and images were captured for further analysis.

Statistical analysis

Data are presented as mean±SD. Statistical comparisons among groups were performed using one-way analysis of variance (ANOVA) followed by Tukey's multiple comparison test (analyses performed in MS Excel 2019 and validated in Python 3 using SciPy/stats models). Differences were considered statistically significant at $p<0.05$.

RESULTS AND DISCUSSION

Extraction

The plant extract from *Tradescantia spathacea* showed higher yields compared to the Ultrasound-assisted extraction (USE) method. According to the findings, USE extraction was found to be more efficient than traditional extraction methods. The results are summarized in table 2 below.

Biosynthesis of nanoparticles of *Tradescantia spathacea*

Biosynthesis of zinc oxide nanoparticles (ZnO NPs)

A 25 ml extract was rapidly mixed with 0.1 M zinc nitrate hexahydrate and agitated for two hours. After the reaction, the resulting precipitate was left to cool for 24 h. The solution was effectively separated from the precipitate through centrifugation at a speed of 6000 revolutions per minute for a duration of 15 min [44].

Table 2: *Tradescantia spathacea* extracts' colour, consistency, and yield in percentage

Plant extract	Colour in daylight	Consistency	Conventional method outcome (% w/w)	Extraction with ultrasound (% w/w)
Methanolic extract	Dark green	Semisolid	10.52	16.29
Ethyl acetate extract	Light green	Semisolid	6.23	8.56
Hydro-alcoholic extract	Slight dark green	Semisolid	6.56	10.19
Petroleum ether extract	Light green	Semisolid	2.31	7.85
Aqueous extract	Light green	Semisolid	8.25	14.45

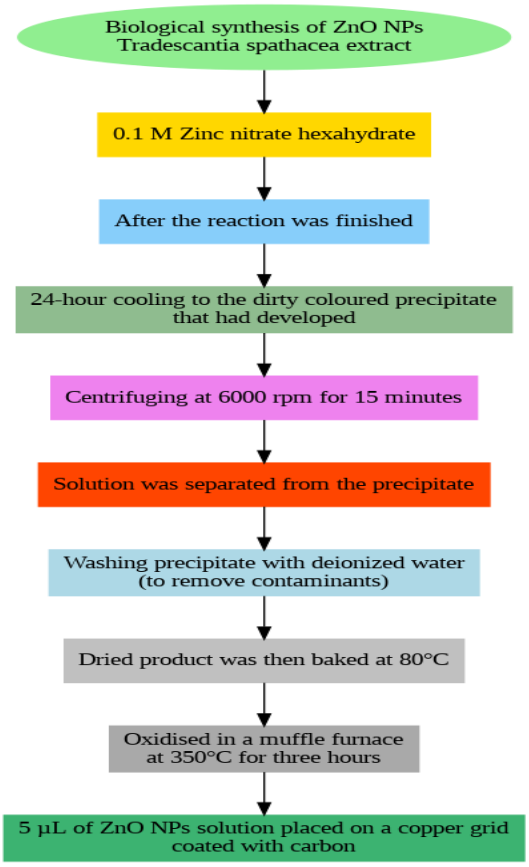

Fig. 1: Biological synthesis of T. S. zinc oxide nanoparticles

The dried product was heated at 80 °C after being periodically rinsed with purified water to remove impurities. Subsequently, five µl of the ZnO nanoparticle solution was added to a carbon-coated copper grid and cooled for three hours at 350 °C in a muffle furnace before SEM analysis (fig. 1).

Characterization of nanoparticles

The biologically synthesized ZnO nanoparticles were characterized using various techniques, including Zeta potential measurement, particle size analysis, scanning electron microscopy (SEM), and X-ray diffraction (XRD).

Particle size and zeta potential

Zeta potential was measured using Dynamic Light Scattering (DLS) from Malvern Instruments. The particle size was determined at 25 °C and a fixed angle of 90°. The nanoparticle dispersion in distilled water was sonicated for 6 min before the analysis. Zeta potential measurements were conducted at 25 °C and 150 V using electrophoretic light scattering. These results also suggested that there is an absence of large aggregates, when these nanoparticles were dispersed in aqueous medium and its supports previous report [45]. The zeta potential indicates the charge conductivity, which helps maintain the stability of the nanoparticle formulation. The nanoparticle size and zeta potential data are shown in fig. 2a and 2b.

a) TSLE-Zn (Particle size)**:** Particle size analysis revealed that the ZnO nanoparticles synthesized using T. S. plant extract have an average mean diameter of 60.91 nm.

b) TSLE-Zn (Zeta potential)**:** Zeta potential measurements for the ZnO nanoparticles synthesized with T. S. plant extract showed a zeta potential value of -0.2 mV, indicating the stability of the nanoparticles in the dispersion. The zeta potential results for *T. S* mediated zinc oxide nanoparticles depicted that synthesized nanoparticles have low stability.

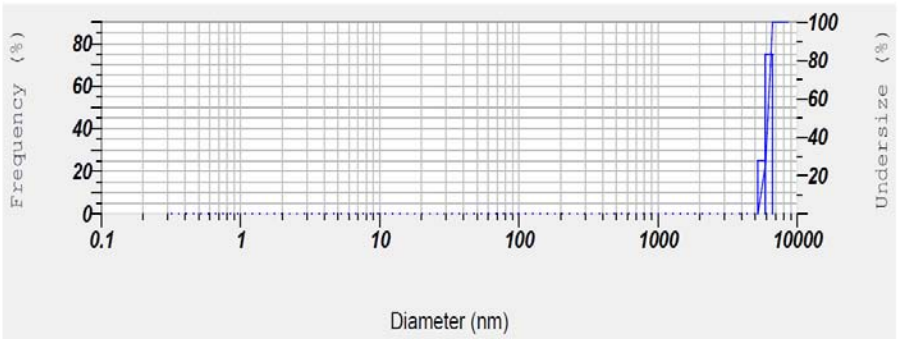

Fig. 2a: TSLE-Zn (Particle size)

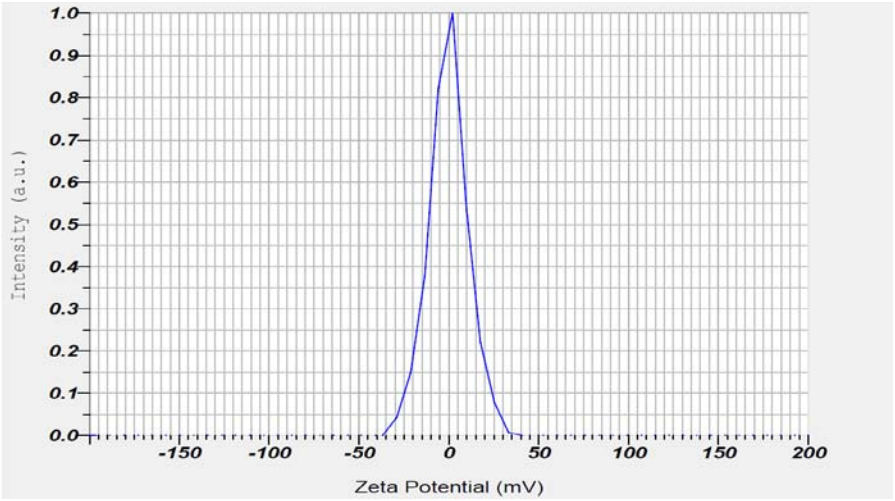

Fig. 2b: TSLE-Zn (Zeta potential)

Fourier transform infrared spectroscopy

The FTIR spectrum of the leaf extract, both before and after the formation of ZnO nanoparticles (NP), was analyzed to identify the functional groups responsible for nanoparticle production. FTIR was used to detect the compounds in the leaf extract that played a role in reducing metal ions and stabilizing the nanoparticle solution. Identifying these functional groups is crucial for understanding the processes involved in nanoparticle synthesis. In this study, the FTIR spectrum of *Tradescantia spathacea*-synthesized ZnO nanoparticles revealed several prominent peaks at 3761, 3817, 2933, 2634, 1635, 1629, and 1383 cm^{-1}. The peaks at 3761, 3817, and 2933 cm^{-1} were likely due to the stretching vibrations of hydroxyl groups (OH) from phenolic compounds or the bending vibrations of hydrogen-bonded functional groups in the leaf extract. These compounds were also discovered to influence ZnO NPs' surface-structure-dependent characteristics. In earlier investigations, similar biomolecules were discovered during the synthesis of ZnO NPs [46]. These peaks could also be attributed to proteins, enzymes, or polysaccharides in the extract, which contribute to the stretching of their (OH) bonds, as shown in fig. 3.

XRD analysis

To assess the dimensional stability of the synthesized nanoparticles, X-ray diffraction (XRD) analysis was performed. The nanoparticles were subjected to testing using a PAN analytical X-ray diffractometer, operating at 4000 volts and a current of 20 mA. The scan was conducted over a 2θ range of 20° to 80° at a rate of 0.02°

per minute, with a 2-time constant for data collection. This analysis allowed for precise determination of the crystal structures and atom positions of the synthesized materials.

Using *Tradescantia spathacea* plant extract, distinct peaks were observed at 2θ values of 44.6°, 64.56°, and 78.9°, corresponding to the (111), (200), (220), and (311) planes of Zn. Additionally, another spectrum displayed peaks at 27.80°, 32.27°, 46.25°, 57.65°, and 78.12°, matching the (111), (200), (220), (311), and (400) planes, respectively. These well-defined XRD patterns confirm the successful synthesis of Zn nanoparticles. The crystalline size of the zinc nanoparticles was influenced by the type of plant extract used in the synthesis process, which may be linked to the therapeutic potential of the extracts. According to the standard values reported in the Joint Committee on Powder Diffraction Standards (correlated to JCPDS) card No. 036-1451, the peaks matched [47]. The compounds within the extracts likely played a role in stabilizing the nanoparticles, potentially acting as capping agents. The XRD results (fig. 4) highlight the importance of the extracts in shaping the properties of the synthesized Zn nanoparticles.

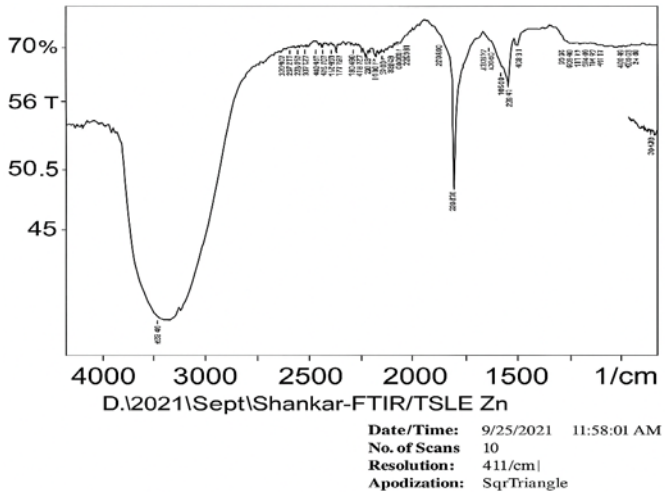

Fig. 3: TSLE Zn ONP: Fourier transform infrared spectroscopy

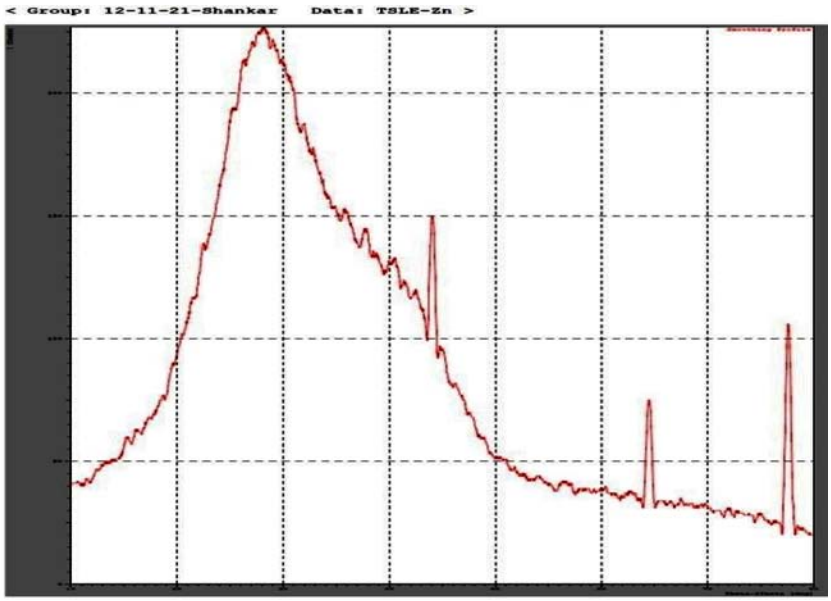

Fig. 4: TSLE Zn ONP: XRD analysis

Scanning electron microscopic (SEM) analysis

Mirror-light microscopes and scanning electron microscopes (SEMs) operate on similar principles. In SEM, an electron beam strikes the surface of a target sample, causing electrons to be reflected. These reflected electrons are detected and converted into an image. In this study, the plant extract was used as a capping agent in the synthesis of nanoparticles. According to the SEM analysis, the zinc oxide nanoparticles derived from *Tradescantia spathacea* are well-dispersed, with individual particles clearly visible. A similar shape of zinc oxide nanoparticles was observed earlier by reference [48]. The average size of the zinc oxide particles was found to range from 50 to 75 nm are generally considered suitable for *in vivo* research based on morphology predictions from the SEM images. No signs of agglomeration were observed, and the nanoparticles exhibited a spherical shape.

Acute toxicity study

The experiment complied with OECD recommendations 425, ZnO NP, TSLE and TSLE ZnO NP at a 2000 mg/kg dosage. Neither the treatment group nor the vehicle control group had any fatalities. Throughout the 14 d study, all animals were checked for toxicity.

Table 3: Behavioural pattern for the various nanoparticles of *Tradescantia spathacea*

	30 min				4 h				24 h				48 h				7 d				14 d			
	VC	ZONP	TSLE	TSLE ZONP	VC	ZONP	TSLE	TSLE ZONP	VC	ZONP	TSLE	TSLE ZONP	VC	ZONP	TSLE	TSLE ZONP	VC	ZONP	TSLE	TSLE ZONP	VC	ZONP	TSLE	TSLE ZONP
Skin	UC	UC	UC	UC	UC	UC	UC	UC	UC	UC	UC	UC	UC	UC	UC	UC	UC	UC	UC	UC	UC	UC	UC	UC
Eyes	UC	UC	UC	UC	UC	UC	UC	UC	UC	UC	UC	UC	UC	UC	UC	UC	UC	UC	UC	UC	UC	UC	UC	UC
Salvation	UC	UC	UC	UC	UC	UC	UC	UC	UC	UC	UC	UC	UC	UC	UC	UC	UC	UC	UC	UC	UC	UC	UC	UC
Respiration	UC	UC	UC	UC	UC	UC	UC	UC	UC	UC	UC	UC	UC	UC	UC	UC	UC	UC	UC	UC	UC	UC	UC	UC
Urination (Color)	UC	UC	UC	UC	UC	UC	UC	UC	UC	UC	UC	UC	UC	UC	UC	UC	UC	UC	UC	UC	UC	UC	UC	UC
Faces consistency	UC	UC	UC	UC	UC	UC	UC	UC	UC	UC	UC	UC	UC	UC	UC	UC	UC	UC	UC	UC	UC	UC	UC	UC
Somatomotor activity and behaviour	UC	UC	UC	UC	UC	UC	UC	UC	UC	UC	UC	UC	UC	UC	UC	UC	UC	UC	UC	UC	UC	UC	UC	UC
Sleep	UC	UC	UC	UC	UC	UC	UC	UC	UC	UC	UC	UC	UC	UC	UC	UC	UC	UC	UC	UC	UC	UC	UC	UC
Mucous membrane	UC	UC	UC	UC	UC	UC	UC	UC	UC	UC	UC	UC	UC	UC	UC	UC	UC	UC	UC	UC	UC	UC	UC	UC
Convoulsons and tremours	A	A	A	A	A	A	A	A	A	A	A	A	A	A	A	A	A	A	A	A	A	A	A	A
Itching	A	A	A	A	A	A	A	A	A	A	A	A	A	A	A	A	A	A	A	A	A	A	A	A
Convoulsons and tremours	A	A	A	A	A	A	A	A	A	A	A	A	A	A	A	A	A	A	A	A	A	A	A	A
Coma	A	A	A	A	A	A	A	A	A	A	A	A	A	A	A	A	A	A	A	A	A	A	A	A
Mortality	A	A	A	A	A	A	A	A	A	A	A	A	A	A	A	A	A	A	A	A	A	A	A	A

Here's the heatmap representation of the clinical observations over time: Blue (UC): Unchanged/Normal observations across time points. Red (A): Absence of symptoms like convulsions, coma, etc., consistently reported.; VC-Vehicle control; ZONP-Zinc oxide nanoparticle; TSLE-*Tradescantia spathacea* leaf extract; TSLE ZONP-*Tradescantia spathacea* leaf extract Zinc oxide nanoparticle

Behavioural pattern and body weight

Zn ONP experienced tired and drowsy effects throughout the first 4 h. Both the treatment and vehicle control groups saw a slight rise in body weight during the acute toxicity assessment (fig. 5). There is no significant difference in the animal body weight after giving treatment with Zn O NP, TSLE and TSLE+Zn O NP compared to control on 1st, 7th and 14th d. The results are showed in the fig. 5.

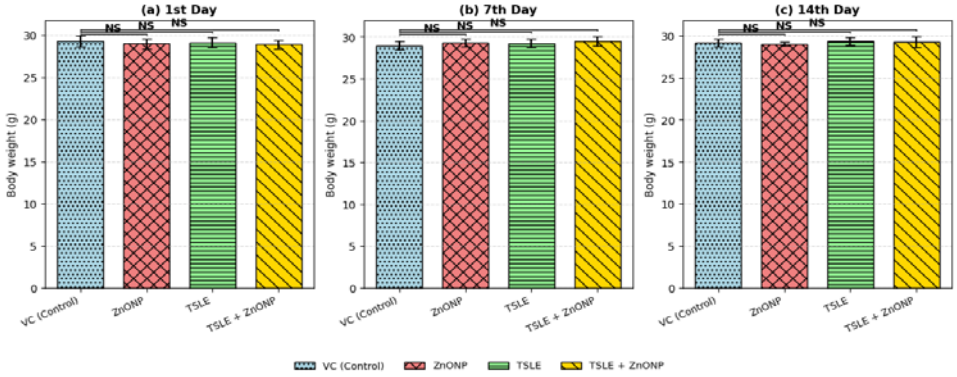

Fig. 5: Effect of *Tradescantia spathacea* leaf extract (TSLE) and its zinc oxide nanoparticles (ZnONPs) on body weight (g) of mice across different treatment groups—VC (Control), ZnONP, TSLE, and TSLE+ZnONP—on the 1st, 7th, and 14th d. Data are expressed as Mean±SD (n = 5). "NS" denotes no statistically significant difference compared to the control group

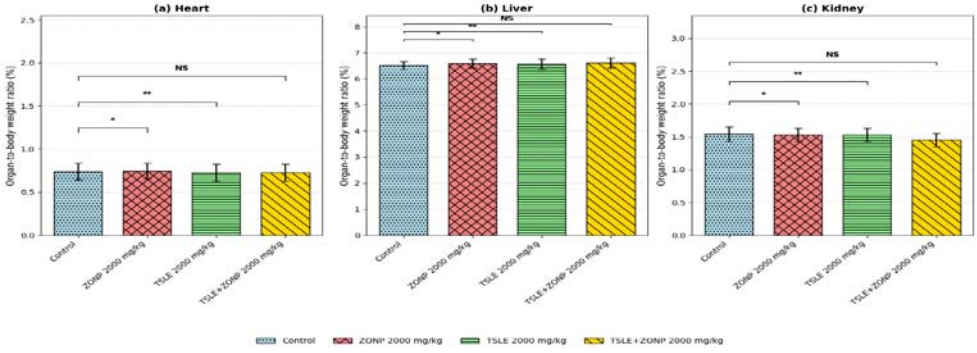

Fig. 6: Organ-to-body weight ratio (%) for Heart, Liver, and Kidney across different treatment groups (Control, ZONP 2000 mg/kg, TSLE 2000 mg/kg, and TSLE+ZONP 2000 mg/kg). Data are expressed as mean±SD (n = 5). Statistical analysis was performed using one-way ANOVA followed by Tukey's post hoc test. Significance levels compared to the Control group are indicated by asterisks: * p<0.05, and ** p<0.01. A single asterisk (*) for (p<0.05) means the result is statistically significant at the 5% level, and a double asterisk (**) for (p<0.01) is significant at the 1% level. NS indicates no statistically significant difference.

Body-organ ratio index

In either group, organ-to-body weight index did not very much. At a p. o. of 2000 mg/kg, no damage was found at the organ level in any of the groups (fig. 6)**.** There is no significant difference in the Body-organ ratio index after giving treatment with ZnONP, TSLE and TSLE+ZnONP compared to control on 1st, 7th and 14th day. The results are showed in the fig. 6.

Biochemical analysis

Tradescantia spathacea leaf extract and *Tradescantia spathacea* leaf extract Zn ONP's increase total cholesterol, LDL, urea, creatinine, albumin, and TSLE and TSLE Zn ONP when compared to the vehicle control. Additionally, globulin and HDL levels dramatically improved in TSLE and TSLE Zn ONP and globulin levels. The biochemical results show that *Tradescantia spathacea* leaf extract and *Tradescantia spathacea* leaf extract Zn ONP's "to avoid over-generalization since changes were not statistically significant" to avoid over-generalization since changes were not statistically significant, in albino mice at 2000 mg/kg, but no serious organ damage (table 4).

Haematological analysis

Tradescantia spathacea leaf extract and *Tradescantia spathacea* leaf extract Zn ONP's, induce considerable increases in HGB, HCT, RBC, MCV, MCH, MCHC, MPV, PLT, and P-LCR levels. WBC and PCT levels rise significantly in TSLE Zn ONPs. In albino mice, *Tradescantia spathacea* leaf extract and *Tradescantia spathacea* leaf extract Zn ONP's caused either minor poisoning or no symptoms, according to a hematologic investigation (table 5).

Table 4: Biochemical evaluation of *Tradescantia spathacea* nanoparticles and extracts in mice

Parameter	Units	VC (Control)	ZnONP (2000 mg/kg)	TSLE (2000 mg/kg)	TSLE + ZnONP (2000 mg/kg)
Carbohydrate metabolism					
Glucose	mg/dl	93.70±1.72	95.32±3.00	95.46±2.34	93.50±2.47
Lipid profile					
Total Cholesterol	mg/dl	98.37±3.04	106.97±1.97	117.35±1.92	117.16±2.05
HDL Cholesterol	mg/dl	30.70±1.72	32.47±2.65	30.42±1.15	42.88±2.21
LDL Cholesterol	mg/dl	45.36±1.21	64.88±2.55	54.43±3.34	51.42±1.70
VLDL Cholesterol	mg/dl	22.43±0.79	24.22±1.02	23.56±1.37	22.72±1.29
Triglycerides	mg/dl	111.92±2.47	124.53±3.32	122.36±4.69	122.03±4.54
CHOL/HDL Ratio	-	3.21±0.20	3.24±0.24	3.86±0.19	3.68±0.23
LDL/HDL Ratio	-	1.48±0.07	1.98±0.18	1.79±0.08	1.61±0.19
Renal function markers					
Urea	mg/dl	37.32±1.84	48.06±1.52	47.85±1.66	43.06±1.42
Creatinine	mg/dl	0.547±0.02	0.555±0.02	0.533±0.02	0.527±0.01
Hepatic function markers					
Total Bilirubin (BIT)	mg/dl	0.674±0.06	0.741±0.06	0.744±0.06	0.733±0.06
Direct Bilirubin (BID)	mg/dl	0.265±0.05	0.260±0.05	0.251±0.04	0.250±0.04
Indirect Bilirubin (BII)	mg/dl	0.430±0.02	0.420±0.05	0.424±0.05	0.424±0.05
Total Protein	mg/dl	6.274±0.27	6.354±0.26	6.268±0.22	6.400±0.21
Albumin	mg/dl	2.270±0.08	2.778±0.21	2.745±0.22	2.580±0.24
Globulin	mg/dl	4.010±0.25	3.580±0.32	3.636±0.27	3.496±0.28
A:G Ratio	-	0.568±0.04	0.771±0.10	0.779±0.10	0.784±0.05
SGOT/AST	U/L	95.99±1.62	141.51±1.69	138.89±4.08	137.34±6.29
SGPT/ALT	U/L	65.94±5.32	96.00±4.60	80.99±2.78	80.15±5.39
ALP	U/L	95.69±6.31	126.75±5.45	118.68±4.65	107.39±3.58

Value are expressed as mean±SD (n = 5). TSLE denotes *Tradescantia spathacea* leaf extract and ZnONP represents zinc oxide nanoparticles.

Table 5: Haematological evaluation of *Tradescantia spathacea* nanoformulations in mice

Parameter	Units	VC (Control)	ZnONP (2000 mg/kg)	TSLE (2000 mg/kg)	TSLE + ZnONP (2000 mg/kg)
Erythrocytic indices					
HGB	g/dL	13.35±0.07	14.37±0.09	13.36±0.05	13.37±0.09
RBCs	10?/?L	8.48±0.07	9.21±0.05	9.11±0.03	9.10±0.04
HCT	%	45.20±0.76	49.76±0.08	45.62±0.20	45.74±0.21
MCV	fL	52.77±1.08	53.69±0.14	52.42±0.10	51.52±0.18
MCH	pg	15.69±0.11	15.73±0.05	15.19±0.02	15.20±0.02
MCHC	g/dl	29.88±0.05	29.47±0.01	30.20±0.10	30.20±0.11
RDW–SD	fL	19.69±0.10	22.05±0.43	21.47±1.20	21.35±0.10
RDW–CV	%	19.11±0.05	19.19±0.06	19.77±0.09	19.88±0.03
Leukocytic indices					
WBCs	10^3/?L	4.956±0.04	4.944±0.02	4.796±0.02	4.822±0.11
NEUT %	%	20.45±0.41	20.84±0.28	20.80±0.34	20.81±0.41
LYMPH %	%	76.39±0.33	75.62±0.35	74.92±0.42	75.11±0.53
MONO %	%	1.01±0.12	1.43±0.09	1.51±0.07	1.51±0.07
EO %	%	2.19±0.12	2.75±0.09	2.64±0.05	2.65±0.08
BASO %	%	0.00±0.00	0.00±0.00	0.00±0.00	0.00±0.00
IG %	%	0.00±0.00	0.00±0.00	0.00±0.00	0.00±0.00
NEUT	10^3/?L	1.01±0.02	1.02±0.04	1.00±0.03	1.01±0.04
LYMPH	10^3/?L	3.78±0.04	3.79±0.04	3.61±0.01	3.60±0.01
MONO	10^3/?L	0.056±0.01	0.076±0.01	0.077±0.01	0.077±0.01
EO	10^3/?L	0.116±0.01	0.138±0.00	0.138±0.00	0.138±0.00
BASO	10^3/?L	0.00±0.00	0.00±0.00	0.00±0.00	0.00±0.00
IG	10^3/?L	0.00±0.00	0.00±0.00	0.00±0.00	0.00±0.00
Platelet indices					
PLT	10^3/?L	693.49±2.33	786.40±4.02	765.56±2.02	765.69±2.37
PDW	fL	6.75±0.05	7.16±0.05	6.76±0.05	6.75±0.06

Value are expressed as mean±SD (n = 5). TSLE denotes *Tradescantia spathacea* leaf extract, and ZnONP represents zinc oxide nanoparticles

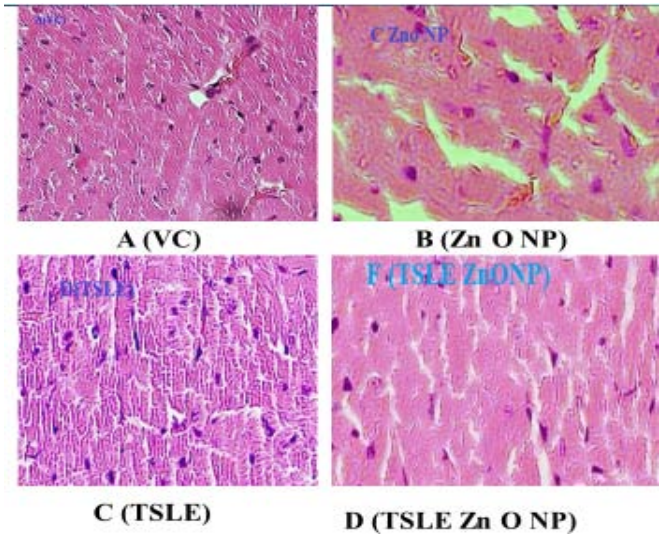

Fig. 7: Heart histopathological observations, A (VC): Nothing abnormal detected; B (ZnONP): Moderate myocardial fatty fiber infiltration; C (TSLE): Moderate myocardial fatty fiber infiltration; D (TSLE Zn ONP): Have mild granular degeneration

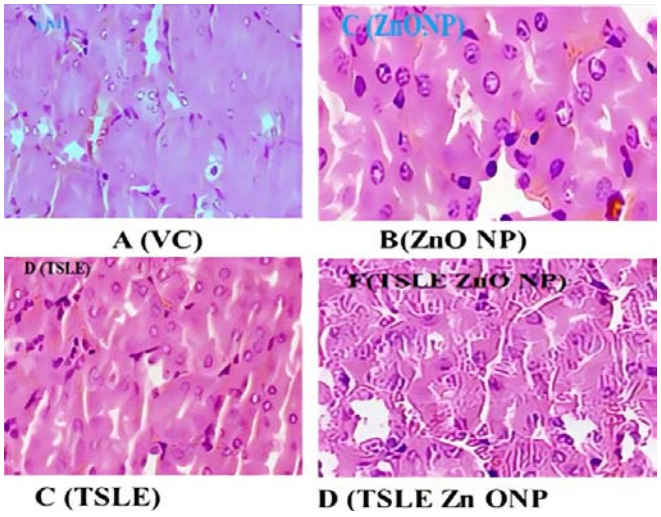

Fig. 8: Kidney histopathological observations, A (VC): There is no growth in tissues; B (Zn ONP): Moderate tubular epithelial cell degeneration; C (TSLE): Mild tubular epithelial cell degeneration; D (TSLE Zn ONP): Moderate tubular epithelial cell necrosis and granular degeneration

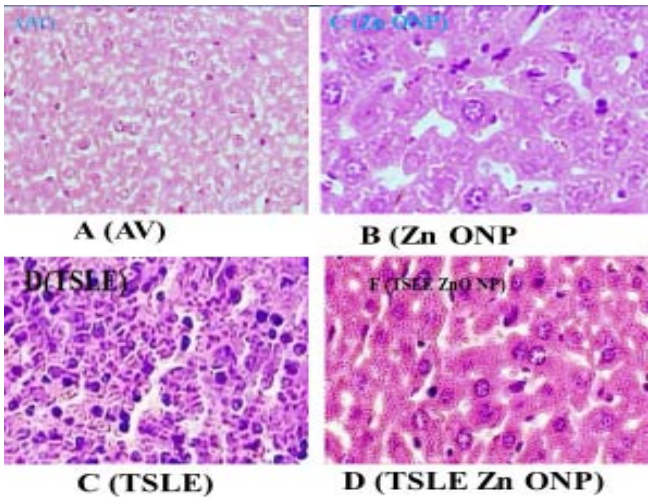

Fig. 9: Observations on liver histopathology, A (VC): There is no growth in tissues; B (Zn O NP): Hepatocytes of the liver with Moderate granular degeneration; C (TSLE): Mild liver hepatocyte granular degeneration; D (TSLE Zn O NP): Hepatocytes of the liver with Mild to moderate granular degeneration

Histopathology analysis

At 2000 mg/kg, p. o., TSLE Zn ONP, and TSLE Extract NPs did not show serious organ markers of toxicity. Fig. 7, 8, and 9 summarise the cardiac, kidney, and liver histology findings. According to the findings, TSLE Zn ONP, and TSLE NPs only have a mildly toxic effect on the heart, liver, and kidney.

However, TSLE Zn ONPs have a showed mild, reversible cellular changes without overt toxicity effect on the organ level. Research on biochemical and haematological variables and the organ-to-body weight index supports these results. According to the findings of acute oral toxicity tests, ZnO NPs at 2000 mg/kg b. w. did not cause any deaths while under treatment [48]. All plant NPs are thus classified as having acute oral toxicity as category 5 under the GHS (Globally Harmonized System of Classification category).

DISCUSSION AND CONCLUSION

The present study demonstrated the successful green synthesis of zinc oxide nanoparticles (ZnO NPs) using the methanolic leaf extract of *Tradescantia spathacea*. Characterization by XRD confirmed the hexagonal crystalline structure, while SEM revealed uniformly distributed spherical nanoparticles (50–75 nm). The zeta potential (−0.2 mV) and FTIR peaks indicated that phenolic and hydroxyl groups acted as stabilizing and capping agents, supporting controlled nanoparticle formation.

Acute oral toxicity studies conducted as per OECD 425 guidelines revealed no mortality or behavioral abnormalities in mice treated with ZnONP, TSLE, or TSLE+ZnONP (2000 mg/kg). Body weight, organ-to-body weight ratios, and clinical signs remained normal throughout the 14-day observation period. Biochemical and hematological analyses indicated only mild and reversible variations within physiological limits, suggesting negligible hepatic or renal toxicity. Histopathological evaluation showed minor granular degeneration without necrosis or structural distortion in liver, kidney, and heart tissues, confirming biocompatibility. These findings align with previous reports on plant-mediated ZnO nanoparticles, emphasizing the safety of biologically synthesized nanomaterials. The *T. spathacea* phytochemicals not only facilitated nanoparticle stabilization but may also have contributed to antioxidant and immunomodulatory effects reflected in improved HDL and globulin levels [49].

In conclusion, *Tradescantia spathacea*-mediated ZnO nanoparticles are structurally stable, safe up to 2000 mg/kg, and environmentally benign. Their biosafety profile supports future pharmacological applications, particularly in antioxidant, hepatoprotective, and antidiabetic therapies, highlighting their potential as promising agents in green nanomedicine.

ACKNOWLEDGMENT

I am grateful to Lovely Professional University, Jalandhar, Punjab, India, for their advice, kindness, and encouragement throughout my career.

FUNDING

This research did not receive any specific grant from funding agencies in the public, commercial, or not-for-profit sectors.

ABBREVIATIONS

ANOVA — Analysis of Variance; CMC — Carboxymethyl Cellulose; DLS — Dynamic Light Scattering; FL — Femtoliters; FTIR — Fourier transform infrared spectroscopy; LD50 — Lethal Dose 50%; MCV — mean Corpuscular Volume; NP — Nanoparticles; NPD — Normal Pellet Diet; OECD — Organization for Economic Co-operation and Development; PDW — Platelet Distribution Width; SEM — scanning electron microscopy; T. S. — *Tradescantia spathacea*; TSLE — *Tradescantia spathacea* Leaf Extract; TSLE ZONP —*Tradescantia spathacea* Leaf Extract Zinc Oxide Nanoparticles; USE — Ultrasound-assisted extraction; XRD — X-ray diffraction; ZnO — Zinc Oxide; ZONP — Zinc Oxide Nanoparticles

AUTHORS CONTRIBUTIONS

Shankaraiah Pulipaka: Investigation, Methodology, Writing –original draft, Ashish Suttee: Conceptualization, Resources, Supervision, R. Vani: review, editing and V. Jyothi: Validation with formal analysis.

CONFLICT OF INTERESTS

The authors declare no conflict of interest.

REFERENCES

1. Al Darwesh MY, Ibrahim SS, Mohammed MA. A review on plant extract-mediated green synthesis of zinc oxide nanoparticles and their biomedical applications. Results Chem. 2024 Feb;7:101368. doi: 10.1016/j.rechem.2024.101368.
2. Joesna G, Alodhayb A, Sasikumar P, Sree TL, Ferin RZ, Sankar D. Biosynthesis zinc oxide nanoparticle: Azadirachta indica and Phyllanthus acidus mediated green approach for enhanced biological efficacy. Chemical Physics Impact. 2025;10:100821. doi: 10.1016/j.chphi.2025.100821.
3. Hamed R, Obeid RZ, Abu Huwaij R. Plant-mediated green synthesis of zinc oxide nanoparticles: an insight into biomedical applications. Nanotechnol Rev. 2023;12(1):20230112. doi: 10.1515/ntrev-2023-0112.
4. Abdelbaky AS, Abd El Mageed TA, Babalghith AO, Selim S, Mohamed AM. Green synthesis and characterization of ZnO nanoparticles using *Pelargonium odoratissimum (L.)* aqueous leaf extract and their antioxidant, antibacterial and anti-inflammatory activities. Antioxidants (Basel). 2022;11(8):1444. doi: 10.3390/antiox11081444, PMID 35892646.
5. Arumugam A, Karthikeyan C, Haja Hameed AS, Gopinath K, Gowri S, Karthika V. Synthesis of cerium oxide nanoparticles using *Gloriosa superba L.* leaf extract and their structural, optical and antibacterial properties. Mater Sci Eng C Mater Biol Appl. 2015;49:408-15. doi: 10.1016/j.msec.2015.01.042, PMID 25686966.
6. Zavitri NG, Syahbaniati AP, Primastuti RK, Putri RM, Damayanti S, Wibowo I. Toxicity evaluation of zinc oxide nanoparticles green synthesized using papaya extract in zebrafish. Biomed Rep. 2023;19(6):96. doi: 10.3892/br.2023.1678, PMID 37901875.
7. Fernandes CA, Jesudoss MN, Nizam A, Krishna SB, Lakshmaiah VV. Biogenic synthesis of zinc oxide nanoparticles mediated by the extract of *Terminalia catappa* fruit pericarp and its multifaceted applications. ACS Omega. 2023;8(42):39315-28. doi: 10.1021/acsomega.3c04857, PMID 37901498.
8. Elumalai K, Velmurugan S, Ravi S, Kathiravan V, Ashokkumar S. Bio-fabrication of zinc oxide nanoparticles using leaf extract of curry leaf (Murraya koenigii) and its antimicrobial activities. Mater Sci Semicond Process. 2015;34:365-72. doi: 10.1016/j.mssp.2015.01.048.
9. Bhuyan T, Mishra K, Khanuja M, Prasad R, Varma A. Biosynthesis of zinc oxide nanoparticles from Azadirachta indica for antibacterial and photocatalytic applications. Mater Sci Semicond Process. 2015;32:55-61. doi: 10.1016/j.mssp.2014.12.053.
10. Murali M, Gowtham HG, Shilpa N, Singh SB, Aiyaz M, Sayyed RZ. Zinc oxide nanoparticles prepared through microbial-mediated synthesis for therapeutic applications: a possible alternative for plants. Front Microbiol. 2023 Sep;14:1227951. doi: 10.3389/fmicb.2023.1227951, PMID 37744917.
11. Maher S, Nisar S, Aslam SM, Saleem F, Behlil F, Imran M. Synthesis and characterization of ZnO nanoparticles derived from biomass (Sisymbrium irio) and assessment of potential anticancer activity. ACS Omega. 2023;8(18):15920-31. doi: 10.1021/acsomega.2c07621, PMID 37179630.
12. Rajendran NK, George BP, Houreld NN, Abrahamse H. Synthesis of zinc oxide nanoparticles using rubus fairholmianus root extract and their activity against pathogenic bacteria. Molecules. 2021;26(10):3029. doi: 10.3390/molecules26103029, PMID 34069558.
13. El Beltagi HS, Rageb M, El Saber MM, El Masry RA, Ramadan KM, Kandeel M. Green synthesis characterization and hepatoprotective effect of zinc oxide nanoparticles from *Moringa oleifera* leaves in CCl_4-treated albino rats. Heliyon. 2024;10(9):e30627. doi: 10.1016/j.heliyon.2024.e30627, PMID 38765133.
14. Haddi R, El Kharraz AM, Kerroumi MI. Green synthesis of zinc oxide nanoparticles using *Pistacia lentiscus L.* leaf extact and evaluating their antioxydant and antibacterial properties. Nano Biomed Eng. 2024;16(2):232-47. doi: 10.26599/NBE.2024.9290056.
15. Carp O, Tirsoaga A, Jurca B, Ene R, Somacescu S, Ianculescu A. Biopolymer starch mediated synthetic route of multi-spheres

and donut ZnO structures. Carbohydr Polym. 2015;115:285-93. doi: 10.1016/j.carbpol.2014.08.061, PMID 25439897.
16. Idaka E, Ogawa T, Kondo T, Goto T. Isolation of highly acylated anthocyanins from Commelinaceae plants Zebrina pendula Rhoeo spathacea and Setcreasea purpurea. Agric Biol Chem. 1987;51(8):2215-20. doi: 10.1080/00021369.1987.10868340.
17. Gonzalez Avila M, Arriaga Alba M, De La Garza M, Del Carmen Hernandez Pretelin M, Dominguez Ortiz MA, Fattel Fazenda S. Antigenotoxic antimutagenic and ROS scavenging activities of a Rhoeo discolor ethanolic crude extract. Toxicol *In Vitro*. 2003;17(1):77-83. doi: 10.1016/s0887-2333(02)00120-0, PMID 12537965.
18. Andrade Cetto A, Cruz EC, Cabello Hernandez CA, Cardenas Vazquez R. Hypoglycemic activity of medicinal plants used among the Cakchiquels in Guatemala for the treatment of type 2 diabetes. Evid Based Complement Alternat Med. 2019;2019:2168603. doi: 10.1155/2019/2168603, PMID 30713569.
19. Roys R. The ethno-botany of the maya. Tulane: Tulane University of Louisiana; 1931. p. 359.
20. Luciano Montalvo C, Boulogne I, Gavillan Suarez J. A screening for antimicrobial activities of caribbean herbal remedies. BMC Complement Altern Med. 2013;13:126. doi: 10.1186/1472-6882-13-126, PMID 23731467.
21. Gutierrez SL, Chilpa RR, Jaime HB. Medicinal plants for the treatment of "nervios," anxiety and depression in mexican traditional medicine. Rev Bras Farmacognosia. 2014;24(5):591-608. doi: 10.1016/j.bjp.2014.10.007.
22. Moe S, Naing K, Htay M. Herbal medicines used by tuberculosis patients in myanmar. Eur J Med Plants. 2018;22(1):1-10. doi: 10.9734/EJMP/2018/37341.
23. Rosales Reyes T, De La Garza M, Arias Castro C, Rodriguez Mendiola M, Fattel Fazenda S, Arce Popoca E. Aqueous crude extract of Rhoeo discolor, a Mexican medicinal plant decreases the formation of liver preneoplastic foci in rats. J Ethnopharmacol. 2007;115(3):381-6. doi: 10.1016/j.jep.2007.10.022, PMID 18063494.
24. Wei L, Zhang W, Yin L, Yan F, Xu Y, Chen F. Extraction optimization of total triterpenoids from Jatropha curcas leaves using response surface methodology and evaluations of their antimicrobial and antioxidant capacities. Electron J Biotechnol. 2015;18(2):88-95. doi: 10.1016/j.ejbt.2014.12.005.
25. Lamari FN, Papasotiropoulos V, Tsiris D, Bariamis SE, Sotirakis K, Pitsi E. Phytochemical and genetic characterization of styles of wild crocus species from the island of crete greece and comparison to those of cultivated c. sativus. Fitoterapia. 2018;130:225-33. doi: 10.1016/j.fitote.2018.09.003, PMID 30213756.
26. Jayappa MD, Ramaiah CK, Kumar MA, Suresh D, Prabhu A, Devasya RP. Green synthesis of zinc oxide nanoparticles from the leaf stem and *in vitro* grown callus of *Mussaenda frondosa L.*: characterization and their applications. Appl Nanosci. 2020;10(8):3057-74. doi: 10.1007/s13204-020-01382-2, PMID 32421069.
27. Sundrarajan M, Ambika S, Bharathi K. Plant extract-mediated synthesis of ZnO nanoparticles using Pongamia pinnata and their activity against pathogenic bacteria. Adv Powder Technol. 2015;26(5):1294-9. doi: 10.1016/j.apt.2015.07.001.
28. Lakshmi Pravallika P, Krishna Mohan G, Venkateswara Rao K, Shanker K. Biosynthesis characterization and acute oral toxicity studies of synthesized iron oxide nanoparticles using ethanolic extract of Centella asiatica plant. Mater Lett. 2019;236:256-9. doi: 10.1016/j.matlet.2018.10.037.
29. Kavitha K, Sujatha K, Manoharan S. Development characterization and antidiabetic potentials of Nilgirianthusciliatus nees derived nanoparticles. J Nanomedine Biotherapeutic Discov. 2017;7(2):152. doi: 10.4172/2155-983X.1000152.
30. Xu R. Progress in nanoparticles characterization: sizing and zeta potential measurement. Particuology. 2008;6(2):112-5. doi: 10.1016/j.partic.2007.12.002.
31. Mohd Yusof H, Mohamad R, Zaidan UH, Abdul Rahman NA. Microbial synthesis of zinc oxide nanoparticles and their potential application as an antimicrobial agent and a feed supplement in animal industry: a review. J Anim Sci Biotechnol. 2019;10(1):57. doi: 10.1186/s40104-019-0368-z, PMID 31321032.
32. Vijayakumar S, Krishnakumar C, Arulmozhi P, Mahadevan S, Parameswari N. Biosynthesis characterization and antimicrobial activities of zinc oxide nanoparticles from leaf extract of Glycosmis pentaphylla (Retz.) DC. Microb Pathog. 2018;116:44-8. doi: 10.1016/j.micpath.2018.01.003, PMID 29330059.
33. Matinise N, Fuku XG, Kaviyarasu K, Mayedwa N, Maaza M. ZnO nanoparticles via Moringa oleifera green synthesis: physical properties and mechanism of formation. Appl Surf Sci. 2017;406:339-47. doi: 10.1016/j.apsusc.2017.01.219.
34. Ashwini J, Aswathy TR, Achuthsankar SN. Green synthesis and characterization of zinc oxide nanoparticles using *Cayratia pedata* leaf extract. Biochem Biophys Rep. 2021 Jul;26:100995. doi: 10.1016/j.bbrep.2021.100995.
35. Zaheer E, Hassan S, Shareef H, Naz A, Hassan A, Qadeer K. Scanning electron microscopy (SEM) and atomic absorption spectroscopic evaluation of Raphanus sativus L. seeds grown in Pakistan. Pak J Pharm Sci. 2021;34(2):545-52. PMID 34275828.
36. Babulla S, Bhulakshmi PB. Green synthesis of zinc oxide nanoparticles using pterocarpus santalinus leaf extract: antioxidant potential and antibacterial efficacy against pseudomonas cichorii in chrysanthemum. Curr Trends Biotechnol Pharm. 2025 Jun;19(2s):142-8. doi: 10.5530/ctbp.2025.2s.14.
37. Vijaya Kumar R LS, Kumar BR S. Acute and repeated oral toxicity of antidiabetic polyherbal formulation flax seed fenugreek and Jamun seeds in Wistar albino rat. J Diabetes Metab. 2016;7(3):1000656. doi: 10.4172/2155-6156.1000656.
38. Shaban E, Salaheldin K, El Sayed E, Abd El Aziz M, Nasr S, M Desouky H. Evaluation of acute oral toxicity of zinc oxide nanoparticles in rats. Egypt J Chem. 2021;64:4591-600. doi: 10.21608/EJCHEM.2021.80810.4003.
39. Mohammadi A, Hashemi N, Ghassabzadeh M, Sharafi A, Yazdinezhad A, Danafar H. Green synthesis and toxicological evaluation of zinc oxide nanoparticles utilizing Punica granatum fruit peel extract: an eco-friendly approach. Sci Rep. 2025 Jul 1;15(1):20853. doi: 10.1038/s41598-025-05544-6, PMID 40596273.
40. Shanker K, Mohan GK, Hussain MA, Jayarambabu N, Pravallika PL. Green biosynthesis characterization *in vitro* antidiabetic activity and investigational acute toxicity studies of some herbal mediated silver nanoparticles on animal models. Pharmacogn Mag. 2017;13(49):188-92. doi: 10.4103/0973-1296.197642, PMID 28216905.
41. Kotha P, Marella S, Allagadda R, Badri KR, Chippada AR. Evaluation of biochemical mechanisms of anti-diabetic functions of Anisomeles malabarica. Biomed Pharmacother. 2019;112:108598. doi: 10.1016/j.biopha.2019.01.059, PMID 30784908.
42. Juarros Basterretxea J, Aonso Diego G, Postigo A, Montes Alvarez P, Menendez Aller A, Garcia Cueto E. Post-hoc tests in one-way ANOVA: the case for normal distribution. Methodology. 2024;20(2):84-99. doi: 10.5964/meth.11721.
43. Assaad HI, Zhou L, Carroll RJ, Wu G. Rapid publication-ready MS-Word tables for one-way ANOVA. Springer Plus. 2014;3:474. doi: 10.1186/2193-1801-3-474.
44. Sankar R, Manikandan P, Malarvizhi V, Fathima T, Shivashangari KS, Ravikumar V. Green synthesis of colloidal copper oxide nanoparticles using Carica papaya and its application in photocatalytic dye degradation. Spectrochim Acta A Mol Biomol Spectrosc. 2014;121:746-50. doi: 10.1016/j.saa.2013.12.020, PMID 24388701.
45. Ahn J, Ko J, Lee S, Yu J, Kim Y, Jeon NL. Microfluidics in nanoparticle drug delivery; from synthesis to pre-clinical screening. Adv Drug Deliv Rev. 2018;128:29-53. doi: 10.1016/j.addr.2018.04.001, PMID 29626551.
46. Santhoshkumar J, Kumar SV, Rajeshkumar S. Synthesis of zinc oxide nanoparticles using plant leaf extract against urinary tract infection pathogen. Resour Effic Technol. 2017;3(4):459-65. doi: 10.1016/j.reffit.2017.05.001.
47. Obeizi Z, Benbouzid H, Ouchenane S, Yılmaz D, Culha M, Bououdina M. Biosynthesis of zinc oxide nanoparticles from essential oil of Eucalyptus globulus with antimicrobial and anti-

biofilm activities. Mater Today Commun. 2020;25:101553. doi: 10.1016/j.mtcomm.2020.101553.

48. Agarwal H, Soumya Menon, Venkat Kumar S, Rajeshkumar S. Mechanistic study on antibacterial action of zinc oxide nanoparticles synthesized using green route. Chem Biol Interact. 2018;286:60-70. doi: 10.1016/j.cbi.2018.03.008, PMID 29551637.
49. Jayarambabu N, Rao KV, Rajendar V. Biogenic synthesis, characterization acute oral toxicity studies of synthesized Ag and ZnO nanoparticles using aqueous extract of Lawsonia inermis. Mater Lett. 2018;211:43-7. doi: 10.1016/j.matlet.2017.09.082.
50. Pulipaka S, Suttee A, Kumar MR, Kasarla R. Exploration of *in vitro* antidiabetic activity of ZnO NPs and Ag NPs synthesized using methanolic extracts of Alpinia mutica and Tradescantia spathaeca leaves. Int J Pharm Qual Assur. 2023;14(3):464-9. doi: 10.25258/ijpqa.14.3.01.